Single-Crystal X-ray Structure and Magnetic Properties of the Polyoxotungstate Complexes $Na_{16}[M_4(H_2O)_2(P_2W_{15}O_{56})_2]\cdot nH_2O$ (M = Mn^{II}, *n* = 53; M = Ni^{II}, *n* = 52): An Antiferromagnetic Mn^{II} Tetramer and a Ferromagnetic Ni^{II} Tetramer

C. J. Gómez-García,† J. J. Borrás-Almenar,† E. Coronado,*,† and L. Ouahab‡

Departamento de Química Inorgánica, Univ de Valencia, Dr. Moliner 50, 46100 Burjasot, Spain, and Laboratoire de Chimie du Solide et Inorganique Moléculaire, Université de Rennes I-CNRS-URA 1495, Av. Général Leclerc, F-35042 Rennes Cedex, France

Received March 2, 1994®

The Mn^{II} (**1**) and Ni^{II} (**2**) members of the family $[M_4(H_2O)_2(P_2W_{15}O_{56})_2]^{16-}$ (M = Co^{II}, Cu^{II}, Zn^{II}) have been synthesized and characterized by X-ray single-crystal analysis (for **1**) and magnetic measurements. These compounds are isostructural to the Cu^{II} and Zn^{II} derivatives ($Na_{16}[Mn_4(H_2O)_2(P_2W_{15}O_{56})_2]\cdot 53H_2O$ (**1**), triclinic, $P\bar{1}$, a = 14.31(3) Å, b = 14.675(4) Å, c = 20.363(9) Å, α = 83.44(3)°, β = 80.61(7)°, γ = 73.85(6)°, Z = 1; $Na_{16}[Ni_4(H_2O)_2(P_2W_{15}O_{56})_2]\cdot 52H_2O$ (**2**), triclinic, $P\bar{1}$, a = 13.73(2) Å, b = 13.79(1) Å, c = 21.52(7) Å, α = 90.7(2)°, β = 96.5(2)°, γ = 119.1(1)°, Z = 1) and comprise a rhomblike M_4O_{16} group (M = Mn^{II}, Ni^{II}) encapsulated between two fragments of the trivacant Dawson–Wells polyanion $[P_2W_{15}O_{56}]^{12-}$. The crystal structure of the Mn^{II} derivative has been solved and compared with that of the Cu^{II} and Zn^{II} derivatives. The Mn^{II} derivative exhibits antiferromagnetic Mn–Mn exchange interactions (J = –0.7 cm^{-1}, J' = –0.2 cm^{-1}) and an S = 0 ground state. In turn, the Ni^{II} derivative shows ferromagnetic exchange interactions within the Ni_4O_{16} entity (J = 8.3 cm^{-1}, J' = 3.5 cm^{-1}) and an S = 4 ground state, the highest spin state reported in a heteropoly complex. These magnetic properties are discussed in connection with the structure and compared with those of other tetranuclear clusters of manganese and nickel, as well as with the copper derivative of the same series.

Introduction

One of the abilities of the polyoxometalate anions is that of acting as ligands accommodating magnetic clusters of transition metal ions between diamagnetic moieties of these molecular metal oxides.[1] This characteristic, exhibited in particular by polyoxometalates structures that are deficient in one or more MO_6 octahedra, together with the possibility of assembling these complexes, can be exploited in order to isolate clusters containing increasing numbers of exchange-coupled spins, which is one of the most exciting goals in molecular magnetism.

In this frame, the trivacant heteropoly ligands $[PW_9O_{34}]^{9-}$ (derived from the Keggin structure[2]) and $[P_2W_{15}O_{56}]^{12-}$ (derived from the Dawson–Wells structure[3]) have given rise to a rich variety of compounds showing magnetic nuclearities of three,[4,5] four,[6,7] five,[8] six,[9] and nine.[10] Among them, the polyoxometalates formulated as $[M_4(H_2O)_2(XW_9O_{34})_2]^{10-}$ (X = P, As; M = Co^{II}, Cu^{II}, Zn^{II}, Mn^{II}) and $[M_4(H_2O)_2(P_2W_{15}O_{56})_2]^{16-}$ (X = P; M = Co^{II}, Cu^{II}, Zn^{II}) constitute two extensive series of compounds in which a tetranuclear magnetic cluster M_4O_{16} is encapsulated between two trivacant heteropoly fragments. This heteropoly framework guarantees an effective magnetic isolation of the cluster, imposing at the same time a rhomblike geometry for which interesting situations of orbital orthogonality or spin frustration are favored. Thus, the Co^{II} clusters exhibit ferromagnetic exchange interactions, while in the Cu^{II} clusters these

† Departamento de Química Inorgánica.
‡ Laboratoire de Chimie du Solide et Inorganique Moléculaire.
• Abstract published in *Advance ACS Abstracts,* August 1, 1994.

(1) (a) Pope, M. T. *Heteropoly and Isopoly Oxometalates*; Springer-Verlag: Berlin, 1983. (b) Pope, M. T.; Müller, A. *Angew. Chem., Int. Ed. Engl.* **1991**, *30*, 34–48.
(2) Keggin, J. F. *Nature* **1933**, *131*, 908.
(3) Dawson, B. *Acta Crystallogr.* **1953**, *6*, 113.
(4) Compounds of formula $[M_3L_n(XW_9O_{34})_2]^{12-}$ (M = Mn^{II}, Fe^{III}, Cu^{II}, Ni^{II}, Co^{II}, Zn^{II}, Pd^{II}, Ce^{IV}, Zr^{IV}, ...; X = P, As, Si; L = H_2O, NO_3^-, NO_2^-, OH^-, ...) containing trinuclear (homometallic and heterometallic) clusters encapsulated between two A-α (or β) $[XW_9O_{34}]^{9-}$ fragments have, structurally and magnetically, been studied: (a) Robert, F.; Leyrie, M.; Hervé, G. *Acta Crystallogr.* **1982**, *B38*, 358. (b) Knoth, W. H.; Domaille, P. J.; Farlee, R. D. *Organometallics* **1985**, *4*, 62. (c) Knoth, W. H.; Domaille, P. J.; Harlow, R. L. *Inorg. Chem.* **1986**, *25*, 1577. (d) Kokoszka, G. F.; Padula, F.; Goldstein, A. S.; Venturini, E. L.; Azevedo, L.; Siedle, A. R. *Inorg. Chem.* **1988**, *27*, 59. (e) Finke, R. G.; Rapko, B.; Weakley, T. J. R. *Inorg. Chem.* **1989**, *28*, 1573.
(5) It is also possible to find three metallic centers in one Keggin molecule in the series $[SiW_9M_3]^{n-}$ (M = Al, Ga, Cr^{III}, Fe^{III}, Mn^{II}, Co^{II}, Ni^{II}, Cu^{II}): (a) Lun-yu, Q.; Bao-jian, Z.; Jun, P.; Jing-fu, L. *Transition Met. Chem.* **1988**, *13*, 18. (b) Jun, P.; Lun-yu, Q.; Ya-guang, C. *Inorg. Chim. Acta* **1991**, *183*, 157. (c) Jingfu, L.; Ortéga, F.; Sethuraman, P.; Katsoulis, D. E.; Costello, C. E.; Pope, M. T. *J. Chem. Soc., Dalton Trans.* **1992**, 1901. (d) Wassermann, K.; Lunk, H. J.; Palm, R.; Fuchs, J. *Acta Crystallogr.* **1994**, *C50*, 348.
(6) For structural and ^{183}W-NMR studies on the series $[M_4(H_2O)_2(XW_9O_{34})_2]^{10-}$ and $[M_4(H_2O)_2(P_2W_{15}O_{56})_2]^{16-}$ see: (a) Weakley, T. J. R.; Evans, H. T.; Showell, J. S.; Tourné, G. F.; Tourné, C. M. *J. Chem. Soc., Chem. Commun.* **1973**, 139. (b) Finke, R. G.; Droege, M.; Hutchinson, J. R.; Gansow, O. *J. Am. Chem. Soc.* **1981**, *103*, 1587. (c) Finke, R. G.; Droege, M. W. *Inorg. Chem.* **1983**, *22*, 1006. (d) Evans, H. T.; Tourné, G. F.; Tourné, C. M.; Weakley, T. J. R. *J. Chem. Soc., Dalton Trans.* **1986**, 2699. (e) Finke, R. G.; Droege, M. W.; Domaille, P. J. *Inorg. Chem.* **1987**, *26*, 3886. (f) Weakley, T. J. R.; Finke, R. G. *Inorg. Chem.* **1990**, *29*, 1235. We want to thank Prof. T. J. R. Weakley for providing us a reprint of his recent publication with the structure of the Zn^{II} derivative. (g) Finke, R.; Weakley, T. J. R. *J. Chem. Crystallogr.* **1994**, *24*, 123.
(7) Magnetic studies on the series $[M_4(H_2O)_2(XW_9O_{34})_2]^{10-}$ and $[M_4(H_2O)_2(P_2W_{15}O_{56})_2]^{16-}$ have been recently reported: (a) Gómez-García, C. J.; Casañ-Pastor, N.; Coronado, E.; Baker, L. C. W.; Pourroy, G. *J. Appl. Phys.* **1990**, *67*, 5995. (b) Gómez-García, C. J.; Coronado, E.; Borrás-Almenar, J. J. *Inorg. Chem.* **1992**, *31*, 1667. (c) Casañ-Pastor, N.; Bas, J.; Coronado, E.; Pourroy, G.; Baker, L. C. W. *J. Am. Chem. Soc.*, **1992**, *114*, 10380; (d) Gómez-García, C. J.; Coronado, E.; Borrás-Almenar, J. J.; Aebersold, M.; Güdel, H. U.; Mutka, H. *Physica B* **1992**, *180–181*, 238. (e) Gómez-García, C. J.; Coronado, E.; Gómez-Romero, P.; Casañ-Pastor, N. *Inorg. Chem.* **1993**, *32*, 3378. (f) Coronado, E.; Gómez-García, C. J. In *Polyoxometalates: from Platonic Solids to Anti-retroviral activity*; Pope, M. T., Muller, A., Eds.; Kluwer Acad. Pub: Dordrecht, The Netherlands, 1994.
(8) Tourné, C. M.; Tourné, G. F.; Zonnevijlle, F. *J. Chem. Soc., Dalton Trans.* **1991**, 143.
(9) Wasfi, S. H.; Rheingold, A. L.; Kokoszka, G. F.; Goldstein, A. S. *Inorg. Chem.* **1987**, *26*, 2934.
(10) (a) Weakley, T. J. R. *J. Chem. Soc., Chem. Commun.* **1984**, 1406. (b) Galán, J. R.; Gómez-García, C. J.; Borrás, J. J.; Coronado, E. *Adv. Mater.* **1994**, *6*, 221.

0020-1669/94/1333-4016$04.50/0

interactions are antiferromagnetic, although spin frustration gives rise to a ground state which contains the intermediate spin $S = 1$.

With the aim of extending theses series to other magnetically interesting ions, we have recently undertaken the investigation of Ni^{II} and Mn^{II} complexes with the Keggin fragment. In the former case an unexpected polyoxotungstate containing a triangular Ni cluster with ferromagnetic exchange interactions has been obtained,[11] while for the manganese member the usual polyoxoanion structure containing an antiferromagnetic Mn_4O_{16} cluster has been found.[7e] We have also found that, in the the Cu^{II} systems, the Keggin derivative is less stable than the Dawson derivative, giving rise (at $T \geq 60$ °C) to a Keggin-reconstituted heteropolyanion formulated as $[PW_{10}Cu_2(H_2O)_2O_{38}]^{7-}$ which contains pairs of CuO_6 octahedra sharing edges or a vertex.[12] Up to now, in the Dawson series only the Cu^{II} and, very recently, the Zn^{II} derivatives have been structurally characterized.[6f,g] With the aim of enlarging this second series, and answering some of the questions which arose when the structure of the Cu^{II} derivative was solved, we report here the synthesis, X-ray structure, and magnetic characterization of the Mn^{II} and Ni^{II} members of this series (hereafter abbreviated as **1** and **2**, respectively).

Experimental Section

Synthesis. Both compounds were synthesized by a modification of the method reported by Finke et al.[6e] for the Co^{II} and Zn^{II} salts of the series $[M_4(H_2O)_2(P_2W_{15}O_{56})_2]^{16-}$: 2.5-mmol amount of $NiCl_2{\cdot}6H_2O$ (0.5943 g) was added to 50 mL of a 1 M solution of NaCl, and then 4 g of $Na_{12}P_2W_{15}O_{56}{\cdot}18H_2O$ (prepared according to ref. 6e) were slowly added to this green solution, which was heated at 60 °C during several minutes until the solution became transparent. Slowly cooling of this solution gave pale green rhomblike prismatic crystals that were recrystallized from water at room temperature. These crystals are stable in open air. The Mn^{II} derivative was synthesized by a similar method, using 2.5 mmol of $MnCl_2{\cdot}4H_2O$ (0.4948 g) and heating at $T < 50$ °C (the use of the Mn^{II} and Ni^{II} nitrates gives similar results). The orange solution was warm filtered thorough paper and allowed to crystallize at room temperature, resulting in the formation of orange rhombic prismatic crystals. These crystals, very soluble in water, were also recrystallized in water at room temperature. In contrast to the nickel compound, the orange manganese crystals partially decompose and lose crystallinity when extracted from their mother liquor and stand in open air. The IR spectra of both compounds are very similar and closely resemble those showed by the Co^{II}, Cu^{II}, and Zn^{II} derivatives of the same series.[6e] After the compounds were dried several weeks at room temperature, the weight loss at 200 °C corresponds to 53 and 52 water molecules for the Mn^{II} and Ni^{II} compounds, respectively (compared to 53 and 46 in the Cu^{II} and Co^{II} derivatives, respectively). Anal. Calcd for $Na_{16}[Mn_4(H_2O)_2(P_2W_{15}O_{56})_2]{\cdot}53H_2O$: Mn, 2.44; W, 61.22; H_2O, 10.60. Found: Mn, 2.44; W, 61.81; H_2O, 10.63. Anal. Calcd for $Na_{16}[Ni_4(H_2O)_2(P_2W_{15}O_{56})_2]{\cdot}52H_2O$: Ni, 2.61; W, 61.24; H_2O, 10.40. Found: Ni, 2.78; W, 61.86; H_2O, 10.35.

X-ray Crystallography. An orange crystal of the manganese compound having approximate dimensions of $0.97 \times 0.54 \times 0.24$ mm^3 was taken directly with its mother liquor, sealed in a Lindemann glass capillary, and mounted on an Enraf-Nonius CAD4 diffractometer equipped with a graphite crystal, incident beam monochromator. Preliminary examination and data collection were performed with Mo Kα radiation. Cell constants and an orientation matrix for data collection were obtained from least-squares refinement, using the setting angles of 25 reflections. During data collection three standard reflections were measured every 1 h and showed no significant decay. Lorentz, polarization, and a semiempirical absorption correction (ψ-scan method)[13] were applied to the intensity data. Other important features of the crystal data are summarized in Table 1 and Table S3 of the supplementary material. The space group was determined to be $P\bar{1}$ (No. 2).[14] All calculations were performed on a VAX computer using MolEN.[15] The structure was solved by direct methods using MULTAN[16] and was developed with successive full-matrix least-square refinements and difference Fourier syntheses, which showed all the remaining atoms. Only the 8584 reflections with $I \geq 3\sigma(I)$ were used in the refinements. Atomic parameters and selected bond distances and angles for **1** are given in Tables 2–4, respectively. (In order to facilitate structural comparisons we have chosen a labeling scheme analogous to that used in the structure of the Cu^{II} and Zn^{II} derivatives.) A remarkable feature in the structure solution is that, as in the Cu^{II} and Zn^{II} derivatives, we found two complete and identically oriented W_{15} frameworks partly overlapping in the E map of the highest figure of merit. As Weakley and Finke,[6f] we introduced the averaged coordinates of each couple of equivalent W atoms in the two sets. Once this was done, successive Fourier differences showed all the Mn, P, O, and Na atoms (the Na atoms are distributed on 20 sites with refined occupancy factors ranging from 0.4 to 1). Finally, up to 50 water molecules were also found by successive Fourier differences (thermal analysis indicates, as in the Cu^{II} derivative, the presence of 53 molecules of water).

Table 1. Crystallographic Data for $Na_{16}[Mn_4(H_2O)_2(P_2W_{15}O_{56})_2]{\cdot}53H_2O$ (**1**)

chem formula $Mn_4P_4W_{30}O_{167}H_{110}Na_{16}$	fw 9009.72
$a = 14.31(3)$ Å	space group (No.) $P\bar{1}$ (2)
$b = 14.675(4)$ Å	$T = 22$ °C
$c = 20.363(9)$ Å	$\lambda = 0.710\ 73$ Å
$\alpha = 83.44(3)°$	$\rho_{calcd} = 3.679$ g cm^{-3}
$\beta = 80.61(7)°$	$\mu = 221.994$ cm^{-1}
$\gamma = 73.85(6)°$	$R(F_o)^a = 0.071$
$V = 4042(8)$ Å^3	$R_w(F_o)^b = 0.093$
$Z = 1$	

$^a R = \sum||F_o| - |F_c||/\sum|F_o|$. $^b R_w = (\sum w(|F_o| - |F_c|)^2/\sum w|F_o|^2)^{1/2}$.

Spectral and Magnetic Measurements. IR spectra were recorded on a Perkin-Elmer 882 IR spectrophotometer. The magnetic measurements were carried out on crystalline powder samples with a magnetometer (905 VTS, SHE Corp.) equipped with a SQUID sensor. The temperature range was 2–300 K, and the magnetic field was 0.1 T. The experimental susceptibility data were corrected in order to obtain an approximately constant value of the $\chi_m T$ product at high temperatures (above 200 K). These corrections account for diamagnetism of the samples and temperature-independent paramagnetism (TIP) contributions.

Structural Results

Crystal Structure of $Na_{16}[Mn_4(H_2O)_2(P_2W_{15}O_{56})_2]{\cdot}53H_2O$ (1). The $[Mn_4(H_2O)_2(P_2W_{15}O_{56})_2]^{16-}$ anion has the general structure proposed earlier for the $[M_4(H_2O)_2(P_2W_{15}O_{56})_2]^{16-}$ series and confirmed recently by Weakley and Finke for the Cu^{II} and Zn^{II} derivatives[6f,g] (Figures 1a and 2): Two α-$P_2W_{15}O_{56}^{-12}$ units each share seven oxygen atoms (one with P2) with a central set of four edge-sharing MnO_6 octahedra. The four Mn atoms lie in the same plane and form a centrosymmetric regular rhomblike cluster with sides of 3.288(7) and 3.291(6) Å, a shortest diagonal of 3.352(7) Å, and angles between Mn atoms very close to 60 and 120° (Figure 1b). The anion has a charge of −16, since two water molecules (O70) are coordinated to two Mn atoms, all the other oxygens (O1–O56) being oxide ions. Other structural features and comparisons with the series $[M_4(H_2O)_2(PW_9O_{34})_2]^{10-}$ have been very clearly established by Weakley and Finke.[6f,g] Nevertheless, there are some new interesting features that are worthwhile to compare with the Cu^{II} and Zn^{II} congeners in order to answer some of the questions arisen when its structure was solved:

(1) The most important difference between the Cu^{II} complex, on one hand, and the Mn^{II} and Zn^{II} complexes, on the other, is, as expected, the absence of Jahn–Teller distortions in the MO_6

(11) Gómez-García, C. J.; Coronado, E.; Ouahab, L. *Angew. Chem., Int. Ed. Engl.* **1992**, *31*, 649.
(12) Gómez-García, C. J.; Coronado, E.; Gómez-Romero, P.; Casañ-Pastor, N. *Inorg. Chem.*, **1993**, *32*, 89–93.
(13) North, A. C. T.; Philips, D. C.; Mathews, F. S. *Acta Crystallogr., Sect. A* **1968**, *24*, 351.
(14) *International Tables for Crystallography*; Hahn, T., Ed.; D. Reidel Pub. Co.: Dordrecht, The Netherlands, 1983; Vol. A (Space Group Symmetry).
(15) MolEN, An Interactive Structure Solution Procedure. Enraf-Nonius, Delft, The Netherlands, 1990.
(16) Main, P.; Germain, G.; Woolfson, F. MULTAN-11/84, a System of Computer Programs for the Automatic Solution of Crystal Structures from X-Ray Diffraction Data. University of York, 1984.

Table 2. Positional and Thermal Parameters for $Na_{16}[Mn_4(H_2O)_2(P_2W_{15}O_{56})_2]\cdot 53H_2O$ (**1**)

atom	*x*	*y*	*z*	B^a (Å^2)	atom	*x*	*y*	*z*	B^a (Å^2)
W1	0.9709(1)	0.13719(9)	0.13269(7)	1.75(3)	O27	0.583(2)	0.372(1)	0.137(1)	2.0(4)*
W2	0.8163(1)	−0.00244(9)	0.19125(7)	1.84(3)	O28	0.822(2)	0.436(1)	0.103(1)	2.0(4)*
W3	0.7563(1)	0.17349(9)	0.06918(7)	1.86(3)	O29	0.901(1)	0.268(1)	0.373(1)	1.5(4)*
W4	0.96380(9)	0.19959(8)	0.30526(6)	1.36(3)	O30	0.771(2)	0.150(1)	0.426(1)	1.8(4)*
W5	0.8136(1)	0.06224(8)	0.36249(7)	1.42(3)	O31	0.488(1)	0.809(1)	0.652(1)	1.4(4)*
W6	0.5811(1)	0.10192(8)	0.29430(7)	1.53(3)	O32	0.546(1)	0.657(1)	0.758(1)	1.4(4)*
W7	0.5213(1)	0.27440(9)	0.17527(7)	1.66(3)	O33	0.641(1)	0.512(1)	0.173(1)	1.3(4)*
W8	0.6882(1)	0.42593(9)	0.11176(6)	1.60(3)	O34	0.830(1)	0.481(1)	0.228(1)	1.4(4)*
W9	0.89916(9)	0.39094(8)	0.17331(6)	1.45(3)	O35	0.943(2)	0.377(1)	0.461(1)	1.8(4)*
W10	0.83452(9)	0.37593(8)	0.43600(6)	1.07(2)	O36	0.692(1)	0.151(1)	0.555(1)	0.8(3)*
W11	0.68387(9)	0.23640(8)	0.49285(6)	1.02(2)	O37	0.388(2)	0.201(2)	0.466(1)	2.4(5)*
W12	0.45345(9)	0.27557(8)	0.42439(6)	1.05(2)	O38	0.289(2)	0.487(1)	0.269(1)	2.1(4)*
W13	0.39293(9)	0.45199(8)	0.30584(6)	1.27(3)	O39	0.508(2)	0.685(2)	0.186(1)	3.3(5)*
W14	0.55828(9)	0.60062(8)	0.24399(6)	1.34(3)	O40	0.854(2)	0.629(2)	0.289(1)	2.3(4)*
W15	0.76908(9)	0.56415(8)	0.30691(6)	1.23(2)	O41	0.692(1)	0.350(1)	0.404(1)	1.1(3)*
Mn1	0.4559(3)	0.3472(3)	0.5857(2)	1.5(1)	O42	0.532(1)	0.380(1)	0.357(1)	1.2(4)*
Mn2	0.6056(3)	0.4819(3)	0.5312(2)	1.23(9)	O43	0.650(1)	0.482(1)	0.316(1)	1.5(4)*
P1	0.7503(6)	0.2355(5)	0.2301(4)	1.3(2)	O44	0.805(1)	0.272(1)	0.495(1)	1.1(3)*
P2	0.6079(5)	0.4270(5)	0.3764(4)	1.0(2)	O45	0.577(1)	0.219(1)	0.455(1)	1.2(4)*
Na1	−0.096(1)	−0.237(1)	0.100(1)	2.7(4)	O46	0.367(1)	0.347(1)	0.368(1)	1.4(4)*
Na2	0.029(2)	−0.145(2)	0.077(2)	7.5(8)	O47	0.477(2)	0.517(1)	0.251(1)	1.8(4)*
Na3	−0.179(2)	0.224(2)	−0.126(1)	5.9(7)	O48	0.680(2)	0.630(1)	0.246(1)	1.9(4)*
Na4	−0.261(2)	−0.119(2)	0.499(1)	7.2(7)	O49	0.834(1)	0.453(1)	0.357(1)	1.3(4)*
Na5	−0.194(3)	0.359(2)	−0.068(2)	12(1)	O50	0.444(1)	0.502(1)	0.569(1)	0.8(3)*
Na6	0.005(2)	0.329(2)	−0.009(1)	9.3(9)	O51	0.505(2)	0.655(1)	0.319(1)	2.0(4)*
Na7	−0.196(3)	−0.118(2)	0.036(2)	8(1)	O52	0.747(1)	0.462(1)	0.485(1)	1.3(4)*
Na8	0.000	0.500	0.500	4.5(7)	O53	0.574(1)	0.634(1)	0.517(1)	0.9(3)*
Na9	0.001(3)	0.363(2)	0.824(1)	10(1)	O54	0.692(1)	0.621(1)	0.375(1)	1.6(4)*
Na10	0.410(2)	0.988(2)	0.508(2)	12(1)	O55	0.636(1)	0.471(1)	0.631(1)	1.1(3)*
O1	1.085(2)	0.103(2)	0.092(1)	3.0(5)*	O56	0.605(1)	0.336(1)	0.538(1)	1.5(4)*
O2	0.838(1)	−0.123(1)	0.189(1)	1.5(4)*	O70	0.461(2)	0.193(2)	0.601(1)	3.0(5)*
O3	0.744(2)	0.162(2)	−0.010(1)	2.7(5)*	O101	0.060(3)	0.432(3)	0.306(2)	8(1)*
O4	0.804(2)	0.163(1)	0.178(1)	1.9(4)*	O102	0.404(3)	0.529(3)	0.110(2)	8(1)*
O5	0.941(2)	0.018(2)	0.153(1)	2.3(4)*	O103	0.938(3)	−0.196(3)	0.312(2)	7(1)*
O6	0.900(2)	0.149(2)	0.059(1)	3.0(5)*	O104	0.138(3)	0.665(3)	0.230(3)	10(1)*
O7	0.775(2)	0.044(2)	0.108(1)	4.0(6)*	O105	0.302(5)	0.047(5)	0.377(4)	17(2)*
O8	0.988(1)	0.134(1)	0.221(1)	1.7(4)*	O106	1.102(4)	−0.085(4)	0.363(3)	12(2)*
O9	0.948(1)	0.268(1)	0.127(1)	1.7(4)*	O107	0.260(5)	−0.070(4)	0.343(3)	16(2)*
O10	0.850(2)	0.007(1)	0.277(1)	1.8(4)*	O108	0.144(3)	0.440(3)	0.015(2)	9(1)*
O11	0.683(1)	0.034(1)	0.227(1)	1.6(4)*	O109	0.408(5)	−0.059(4)	0.382(3)	15(2)*
O12	0.631(2)	0.196(1)	0.115(1)	2.2(4)*	O110	0.528(4)	0.331(4)	−0.014(3)	13(2)*
O13	0.749(1)	0.303(1)	0.068(1)	1.3(4)*	O111	0.164(5)	0.305(5)	0.387(4)	17(2)*
O14	0.805(1)	0.203(1)	0.2911(9)	0.8(3)*	O112	0.166(4)	0.404(4)	0.490(3)	12(2)*
O15	0.642(1)	0.229(1)	0.245(1)	1.5(4)*	O113	0.041(4)	0.901(4)	0.495(3)	11(2)*
O16	0.758(1)	0.332(1)	0.203(1)	0.9(3)*	O114	1.093(2)	−0.459(2)	0.103(2)	5.4(8)*
O17	1.083(2)	0.179(2)	0.314(1)	2.4(5)*	O115	0.281(5)	0.226(5)	0.286(4)	17(2)*
O18	0.836(2)	−0.042(1)	0.415(1)	2.0(4)*	O116	1.226(5)	0.034(5)	0.224(4)	17(2)*
O19	0.470(2)	0.992(2)	0.679(1)	2.3(4)*	O117	0.894(5)	0.234(5)	−0.299(4)	17(2)*
O20	0.434(2)	0.286(2)	0.122(1)	2.8(5)*	O118	1.015(3)	0.574(3)	0.392(2)	8(1)*
O21	0.656(2)	0.491(2)	0.039(1)	2.6(5)*	O119	0.421(4)	0.878(4)	0.275(3)	13(2)*
O22	1.000(2)	0.432(2)	0.139(1)	2.6(5)*	O120	0.646(4)	−0.171(4)	0.273(3)	12(2)*
O23	0.684(1)	0.073(1)	0.347(1)	1.8(4)*	O121	0.776(3)	−0.321(3)	0.119(2)	7(1)*
O24	0.949(1)	0.308(1)	0.246(1)	1.1(3)*	O122	1.123(4)	−0.106(4)	0.202(3)	13(2)*
O25	0.936(1)	0.082(1)	0.349(1)	1.6(4)*	O124	0.821(5)	0.323(5)	0.625(4)	18(3)*
O26	0.507(2)	0.155(1)	0.223(1)	2.1(4)*	O125	0.785(4)	0.547(3)	−0.145(3)	11(1)*

[a] Starred *B* values are for atoms refined isotropically. Anisotropically refined atoms are given in the form of the isotropic equivalent displacement parameter defined as $(4/3)[a^2B(1,1) + b^2B(2,2) + c^2B(3,3) + ab(\cos\gamma)B(1,2) + ac(\cos\beta)B(1,3) + bc(\cos\alpha)B(2,3)]$.

octahedra for the Mn^{II} and Zn^{II} derivatives. Thus, while in the Cu^{II} complex the axial distances (2.31(4)–2.61(4) Å) are significantly larger than the equatorial ones (1.89(3)–2.08(4) Å), in the Mn^{II} and Zn^{II} compounds these distances are more homogeneous: axial distances range from 2.13(2) to 2.24(2) in **1** (2.08(2) to 2.19(2) Å in the Zn^{II} complex), whereas the equatorial ones range from 2.05(2) Å to 2.26(2) Å in **1** (2.02(3) to 2.20(2) Å in the Zn^{II} complex). This feature, already observed in the $[M_4(H_2O)_2(XW_9O_{34})_2]^{10-}$ series, shows the ability of the trivacant polyoxotungstate fragments to accommodate magnetic clusters of different transition metals presenting, or not, structural distortions.

(2) This absence of the Jahn–Teller effect implies other structural differences, already advanced by Weakley and Finke, that are now confirmed. These are as follows.

(i) Although the displacements of the W atoms from the mean plane in the six W belt (W10–W15) closest to the M_4O_{16} cluster are of the same nature, they are bigger in the Cu^{II} complex: W10 and W13 move toward the metallic cluster (0.007–0.015, 0.011–0.012, and 0.034–0.047 Å in the Mn^{II}, Zn^{II}, and Cu^{II} complexes, respectively), whereas W11, W12, W14, and W15 move away from the metallic cluster (0.001–0.010, 0.002–0.010, and 0.005–0.034 Å in the Mn^{II}, Zn^{II}, and Cu^{II} clusters, respectively). In the other six W belt (W4–W9) we observe the same effect (0.001–0.003, 0.003–0.012, and 0.018–0.034 Å in the Mn^{II}, Zn^{II}, and Cu^{II} clusters, respectively). It seems clear that these displacements are due to the presence of the central M_4O_{16} cluster and, consequently, they are bigger in the Cu^{II} compound as a result of the Jahn–Teller distortions in the Cu_4O_{16} cluster. In all cases the four mean planes formed by three W (W1–W3), six W (W4–

Table 3. Bond Distances (Å) for $Na_{16}[Mn_4(H_2O)_2(P_2W_{15}O_{56})_2]\cdot 53H_2O$ (1)[a]

W1–O1	1.67(2)	W10–O44	1.93(2)
W1–O4	2.36(2)	W10–O49	1.86(2)
W1–O5	1.90(2)	W10–O52	1.78(2)
W1–O6	1.91(3)	W11–O30	1.99(2)
W1–O8	1.85(2)	W11–O36	1.67(2)
W1–O9	1.84(2)	W11–O41	2.32(2)
W2–O2	1.71(2)	W11–O44	1.95(2)
W1–O4	2.37(2)	W11–O45	1.92(2)
W2–O5	1.91(2)	W11–O56	1.82(2)
W2–O7	1.88(3)	W12–O31	2.03(2)
W2–O10	1.91(2)	W12–O37	1.70(2)
W2–O11	1.88(2)	W12–O42	2.34(2)
W3–O3	1.68(3)	W12–O45	1.90(2)
W3–O4	2.40(2)	W12–O46	1.86(2)
W3–O6	1.96(2)	W12–O53	1.81(2)
W3–O7	1.94(3)	W13–O32	2.08(2)
W3–O12	1.83(2)	W13–O38	1.71(2)
W3–O13	1.87(2)	W13–O42	2.33(2)
W4–O8	2.00(2)	W13–O46	1.96(2)
W4–O14	2.33(2)	W13–O47	1.88(2)
W4–O17	1.69(2)	W13–O55	1.74(2)
W4–O24	1.87(2)	W14–O33	2.05(2)
W4–O25	1.95(2)	W14–O39	1.70(2)
W4–O29	1.77(2)	W14–O43	2.38(2)
W5–O10	1.95(2)	W14–O47	1.89(2)
W5–O14	2.37(2)	W14–O48	1.91(2)
W5–O18	1.74(2)	W14–O51	1.76(2)
W5–O23	1.90(2)	W15–O34	2.06(2)
W5–O25	1.83(2)	W15–O40	1.72(2)
W5–O30	1.85(2)	W15–O43	2.32(2)
W6–O11	1.96(2)	W15–O48	1.91(2)
W6–O15	2.34(2)	Mn1*–Mn2*	3.288(7)
W6–O19	1.72(2)	Mn2–Mn2*	3.352(7)
W6–O23	1.89(2)	W15–O49	1.91(2)
W6–O26	1.90(2)	W15–O54	1.77(2)
W6–O31	1.77(2)	Mn1–O50	2.23(2)
W7–O12	2.00(2)	Mn1–O51	2.11(2)
W4–O15	2.33(2)	Mn1–O53	2.17(2)
W7–O20	1.74(3)	Mn1–O54	2.08(2)
W7–O26	1.95(2)	Mn1–O56	2.16(2)
W7–O27	1.91(2)	Mn1–O70	2.24(2)
W7–O32	1.77(2)	Mn2–O50	2.26(2)
W8–O13	2.01(2)	Mn2–O50*	2.24(2)
W8–O16	2.36(2)	Mn2–O52	2.05(2)
W8–O21	1.73(2)	Mn2–O53	2.15(2)
W8–O27	1.86(2)	Mn2–O55	2.12(2)
W8–O28	1.93(2)	Mn2–O56	2.13(2)
W8–O33	1.79(2)	P1–O4	1.54(2)
W9–O9	2.03(2)	P1–O14	1.53(2)
W9–O16	2.37(2)	P1–O15	1.55(2)
W9–O22	1.73(2)	P1–O16	1.49(2)
W9–O24	1.90(2)	P2–O41	1.54(2)
W9–O28	1.89(2)	P2–O42	1.56(2)
W9–O34	1.79(2)	P2–O43	1.52(2)
W10–O29	2.07(2)	P2–O50	1.55(2)
W10–O35	1.72(2)	Mn1*–Mn2	3.291(6)
W10–O41	2.37(2)		

[a] Numbers in parentheses are estimated standard deviations in the least significant digits.

Table 4. Selected Bond Angles (deg) between W, Mn, and P atoms for $Na_{16}[Mn_4(H_2O)_2(P_2W_{15}O_{56})_2]\cdot 53H_2O$ (1)[a]

W2–W1–W3	59.88(4)	W1–P1–W2	58.5(1)
W1–W2–W3	60.06(4)	W1–P1–W3	58.7(1)
W1–W3–W2	60.06(4)	W2–P1–W3	58.3(1)
W5–W4–W9	120.34(5)	W4–P1–W5	56.3(1)
W4–W5–W6	119.95(4)	W5–P1–W6	62.9(1)
W5–W6–W7	120.08(5)	W6–P1–W7	56.5(1)
W6–W7–W8	119.89(5)	W7–P1–W8	63.6(1)
W7–W8–W9	120.28(5)	W8–P1–W9	57.0(1)
W4–W9–W8	119.47(5)	W9–P1–W4	63.2(2)
W11–W10–W15	119.96(5)	Mn1–P2*–Mn2*	59.2(2)
W10–W11–W12	119.85(4)	Mn1–P2–Mn2*	59.2(2)
W11–W12–W13	119.84(5)	Mn2–P2–Mn2*	60.4(2)
W12–W13–W14	119.91(5)	W10–P2–W11	57.3(1)
W13–W14–W15	120.07(4)	W11–P2–W12	63.0(1)
W10–W15–W14	120.37(5)	W12–P2–W13	57.2(1)
Mn2–Mn1–Mn2*	61.3(1)	W13–P2–W14	62.3(1)
Mn1*–Mn2–Mn1	118.7(2)	W14–P2–W15	57.2(1)
Mn1–Mn2–Mn2*	59.4(1)	W15–P2–W10	62.3(1)
Mn1*–Mn2–Mn2*	59.3(1)		

[a] Starred atoms are related by the inversion symmetry operation ($-x$, $-y$, $-z$).

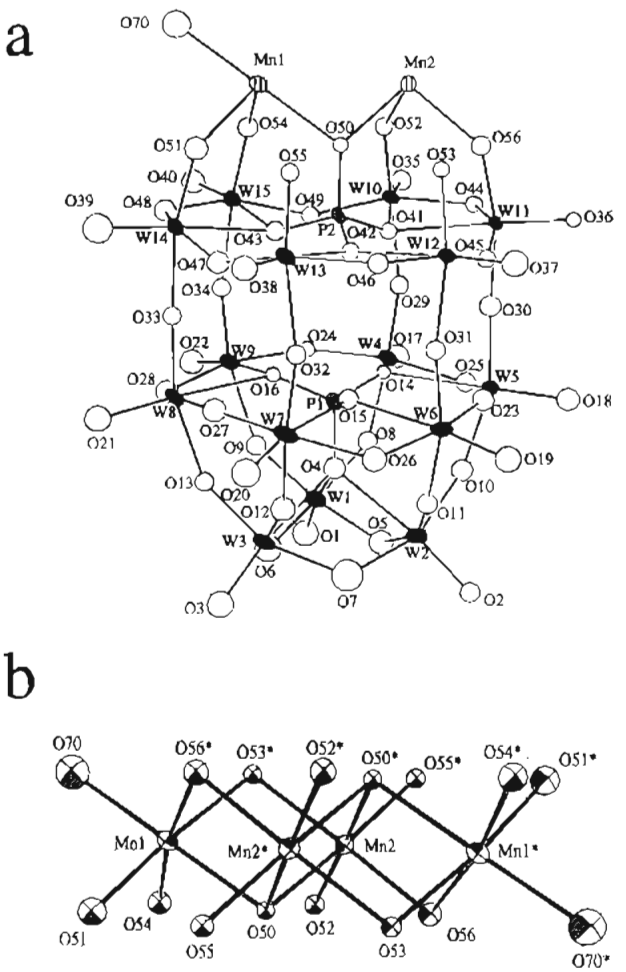

Figure 1. (a) ORTEP drawing of half of the $[Mn_4(H_2O)_2(P_2W_{15}O_{56})_2]^{16-}$ anion (1), showing 50% probability ellipsoids and the labeling scheme. (b) Central tetrameric unit Mn_4O_{16} showing the bridging oxygen atoms and their numbering scheme. (Atoms marked with an asterisk are related by the inversion symmetry operation: $-x$, $-y$, $-z$).

W9), six W (W10–W15), and four M, respectively, remain almost parallel (dihedral angles less than 1°).

(ii) A second difference deals with the geometry of the three metal atoms from the M_4O_{16} cluster capping the trivacant fragment $[P_2W_{15}O_{56}]^{12-}$. In the Cu^{II} derivative, the copper atoms are asymmetrically placed with respect to the normal through P2 to the cluster plane. This situation can be easily seen from the three different P2–Cu distances (3.05(1), 3.19(1), and 3.22(1) Å). On the contrary, in the Mn^{II} and Zn^{II} derivatives, where there are not distortions in the MO_6 octahedra, the three metallic atoms that cap the trivacant fragment are symmetrically placed with respect to the P2 atom and, consequently, the three P2–M distances are almost equal within experimental error, 3.329(9), 3.329(8), and 3.335(9) Å in **1** and 3.27(1), 3.26(1), and 3.29(1) Å in the Zn^{II} complex, confirming, thus, that the Jahn–Teller distortions in the Cu_4O_{16} cluster are responsible for this unsymmetrical arrangement of the P2 atom in the Cu^{II} derivative.

(3) Additionally, we can also note that in all compounds both P atoms of the trivacant polyoxotungstate are significantly displaced, in the same sense, from the mean plane of their corresponding W belts: P1 is displaced away from the M_4O_{16} cluster 0.179, 0.185, and 0.194 Å in the Mn^{II}, Zn^{II}, and Cu^{II}

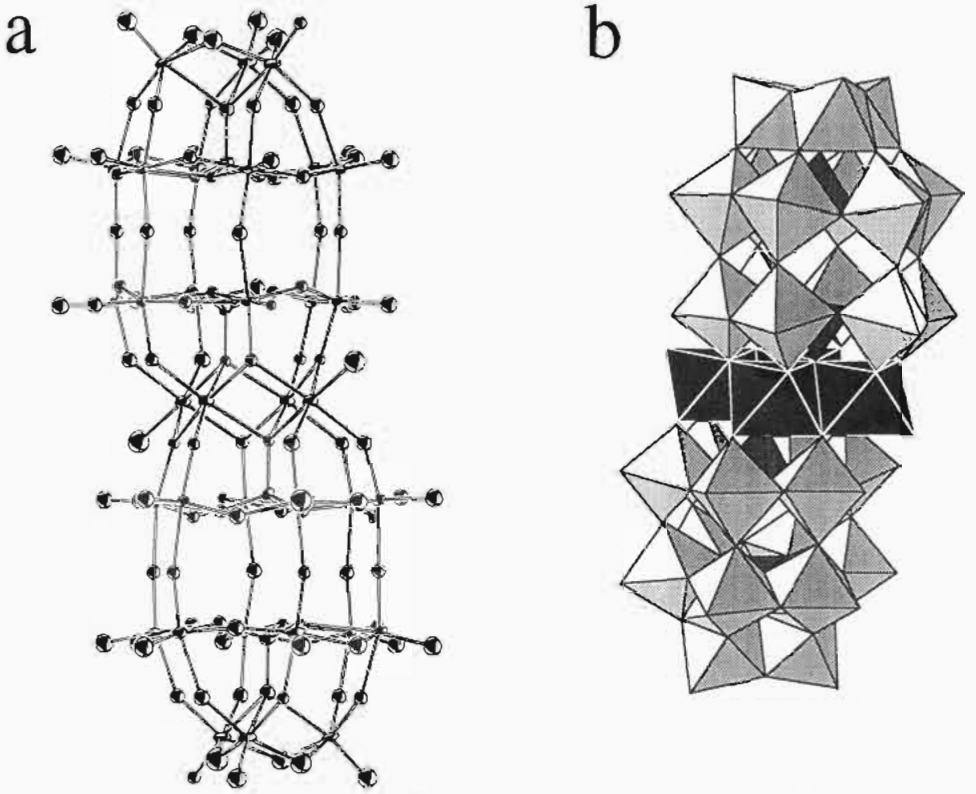

Figure 2. (a) ORTEP drawing of the $[Mn_4(H_2O)_2(P_2W_{15}O_{56})_2]^{16-}$ anion. (b) Polyhedral representation of the same anion. Each octahedron locates a W atom approximately in its center and an oxygen atom in each vertex. The MO_6 octahedra are represented in black. P atoms are located in the four central tetrahedra. The two circles in the Mn_4O_{16} cluster locate the water molecules (O70) coordinated to Mn1 and Mn1*.

derivatives,[17] respectively, whereas P2 is displaced toward the M_4O_{16} cluster 0.222, 0.183, and 0.186 Å in the Mn^{II}, Zn^{II}, and Cu^{II} derivatives, respectively. The small differences in the displacements of the P1 atom in all compounds are expected, since P1 atom is very far from the central cluster. However, the displacements of the P2 atom indicate that they are not only due to the presence/absence of Jahn–Teller distortions in the M_4O_{16} cluster but also to the size of M. This is confirmed by the distance between the mean plane of W atoms (W10–W15) and the central cluster: 2.949, 2.888, and 2.893 Å for the Mn^{II}, Zn^{II}, and Cu^{II} derivatives, respectively (note that the ionic radii are 0.80, 0.74, and 0.69 Å, respectively). Moreover, the P2–O50 distances are equal for the three compounds within experimental error (1.54(2)–1.55(2) Å).

(4) As in the Zn^{II} and Cu^{II} derivatives, in the Mn^{II} compound the bond distances along any sequence of trans-directed bonds $Mn–O–W_{belt}–O–W_{belt}–O–W_{cap}$ are alternatively short and long although the differences decreases as we move away from the central cluster (average distances of 2.12, 1.78, 2.05, 1.79, 1.99, and 1.86 Å). This observation confirms that the deviations are produced by the change in the valence sums[18] when replacing three W^{VI} atoms of one cap by three M^{II}, as suggested by Weakley and Finke.[6f,g]

Despite the usual problems shown by the polyoxometalates salts to locate all cations and water molecules,[19] in **1** all the 16 Na^+ counterions and up to 50 water molecules have been located by difference Fourier maps (thermal analysis indicates 53 water molecules). In any case, the number of water molecules, as in many other polyoxometalates, depends largely on the drying and synthesis conditions and varies from one sample to another.

(17) The values obtained for the Cu^{II} and Zn^{II} derivatives are calculated from the atomic coordinates of these compounds given in ref 6f,g.
(18) Brown, I. D.; Altermatt, D. *Acta Crystallogr., Sect. B* **1985**, *41*, 244.
(19) As pointed out in footnote 13 of ref 6f, the usual disorder in cations and water molecules prevents us to be sure of their numbers and multiplicities in the X-ray structure determination. In the Cu^{II} derivative only 4 of the 14 Na^+ and 18 of the 53 water molecules could be located.

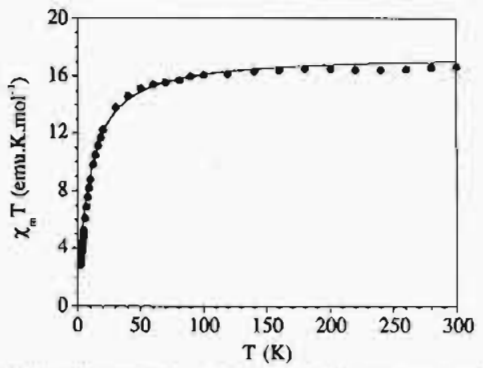

Figure 3. Plot of the product $\chi_m T$ for the Mn^{II} derivative (**1**) at $H = 0.1$ T. The solid line represents the best fit to eq 4.

Magnetic Results

Magnetic Properties of the Manganese Cluster. For **1** the product of the magnetic susceptibility times the temperature ($\chi_m T$) versus the temperature has a constant value of ca. 16.5 emu·K·mol^{-1} from room temperature to ca. 100 K (Figure 3). This value is slightly smaller than the expected value for four noninteracting Mn^{II} ions (17.5 emu·K·mol^{-1}). Between 100 and ca. 30 K $\chi_m T$ drops softly, and below 30 K $\chi_m T$ drops very sharply to reach a value of ca. 2.5 emu·K·mol^{-1} at 2 K. This behavior is indicative of antiferromagnetic exchange interactions between the Mn^{II} ions in the Mn_4O_{16} cluster, leading to a nonmagnetic $S = 0$ ground state. A similar behavior has been very recently observed in the manganese derivative of the $[M_4(H_2O)_2(PW_9O_{34})_2]^{10-}$ series.[7e]

Magnetic Properties of the Nickel Cluster. For **2** a different behavior is observed (see Figure 4): Upon cooling, the product $\chi_m T$ gradually increases from aproximately 5.2 emu·K·mol^{-1} at 300 K to aproximately 6.6 emu·K·mol^{-1} at 70 K. Below this temperature $\chi_m T$ increases more sharply to reach a maximum of ca. 10 emu·K·mol^{-1} at 12 K, and finally it decreases to a value

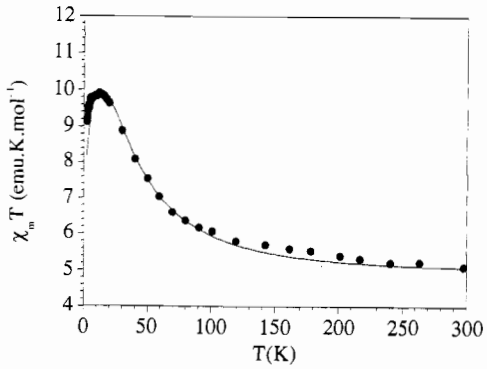

Figure 4. Plot of the product $\chi_m T$ for the Ni^{II} derivative (**2**) at $H = 0.1$ T. The solid line represents the best fit to eq 5.

of ca. 9 emu·K·mol^{-1} at 2 K. This behavior agrees with the presence of ferromagnetic exchange interactions between the four Ni^{II} atoms leading to an $S = 4$ ground state for the cluster.

Analyses of the Magnetic Interactions. Owing to the isotropic ground states of the interacting ions ($^6A_1$ and $^3A_2$ for octahedral Mn^{II} and Ni^{II}, respectively) the magnetic exchange interactions can be described by a Heisenberg-type Hamiltonian:

$$H = -2J(S_1S_2 + S_2S_3 + S_3S_4 + S_4S_1) - 2J'S_2S_4 \quad (1)$$

where J and J' refer to the magnetic exchange interactions of the sides and shortest diagonal of the rhomb according to the numbering scheme

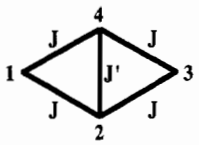

The eigenvalues for the above hamiltonian can be derived from the vector coupling method of Kambé:[20]

$$E(S,S',S'') = -J[S(S+1) - S'(S'+1) - S''(S''+1)] - J'[S'(S'+1) - S_2(S_2+1) - S_4(S_4+1)] \quad (2)$$

where $S = S' + S''$, with $S' = S_2 + S_4$ and $S'' = S_1 + S_3$, and $S_1 = S_2 = S_3 = S_4 = {}^5/_2$ for Mn^{II} and 1 for Ni^{II}. The magnetic susceptibility per mole of tetrameric cluster is given as shown in eq 3. The values for E_i and the coefficients a_i and b_i are summarized in Tables S1 and S2 (supplementary material) for both $s = {}^5/_2$ and $s = 1$ tetranuclear clusters.

$$\chi_{cluster} = \left(\frac{4}{3}\right)\frac{N_a g^2 \mu_B{}^2}{k_B T} s(s+1)\left[\frac{\sum_i a_i \exp(-E_i/k_B T)}{\sum_i b_i \exp(-E_i/k_B T)}\right] \quad (3)$$

The magnetic data of **1** have been fitted to eq 4, where the first term refers to the susceptibility of the cluster and the second one

$$\chi_m = (1-c)\chi_{cluster} + c[(N_a g^2 \mu_B{}^2/3k_B)s(s+1)] \quad (4)$$

to that of a paramagnetic Mn^{II} contribution. In this expression $(1 - c)$ and c are the molar fractions of the Mn_4 clusters and $s = {}^5/_2$ monomeric entities, respectively.

A very satisfying description of the magnetic data over the whole temperature range (solid line in Figure 3) has been obtained from the following set of parameters: $g = 2.0$, $J = -1.2$ cm^{-1}, $J' = -0.2$ cm^{-1}, and $c \approx 0.4$ (approximately 40% of paramagnetic Mn^{II}). This percentage indicates that the compound contains approximately one isolated Mn^{II} ion per Mn_4O_{16} cluster (note that the total number of Mn^{II} ions per mol is 4). The presence of this large amount of paramagnetic Mn^{II} may be related with the instability of the compound. One can imagine for example a progressive decomposition of the polyoxoanion structure releasing paramagnetic species (monosubstituted or trisubstituted Dawson–Wells fragments, Mn^{II} counterions, etc.).[21]

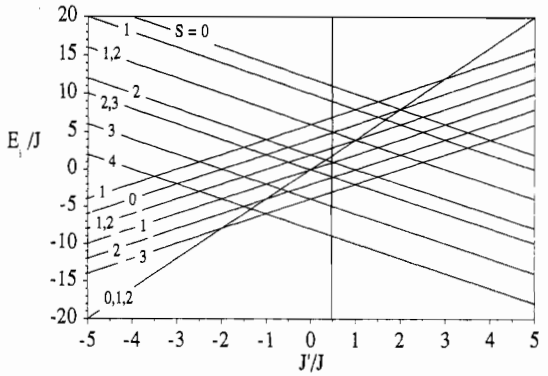

Figure 5. Energy diagram of the different spin states of the Ni^{II} tetramer (as a plot of Ei/J versus J'/J). Numbers on the lines correspond to the total spin values. The vertical line corresponds to the experimental J'/J value found for the present complex ($\approx$0.42).

The two types of exchange parameters are antiferromagnetic and very close to those previously reported ($J = -1.7$ cm^{-1}, $J' = -0.3$ cm^{-1})[7e] for the Keggin derivative $[Mn_4(H_2O)_2(PW_9O_{34})_2]^{10-}$, in agreement with the quasi-identical structural features of the Mn_4O_{16} entity in both compounds, independently of the polyoxotungstate ligand (see Table 5). The weak values of these exchange parameters are comparable to those reported in other Mn^{II} clusters with near 90° superexchange paths.[22]

The magnetic data for **2** have been fitted to the following equation:

$$\chi_m = T/(T-\Theta)\chi_{cluster} \quad (5)$$

where mean field corrections have been introduced in the susceptibility of the nickel(II) cluster to account for the intercluster interactions.

A close agreement with the experiment in the overall temperature range has been obtained from ferromagnetic intracluster Ni–Ni interactions, $J = 8.3$ cm^{-1} and $J' = 3.5$ cm^{-1}, and weak antiferromagnetic intercluster interactions, $\Theta = -0.65$ K (solid line in Figure 4). The energy diagram for this kind of cluster is shown in Figure 5 in the case of ferromagnetic exchange interactions in the sides of the rhomb. As can be seen, the ground spin state is the ferromagnetic one, $S = 4$, when both kinds of interactions are ferromagnetic or when the ferromagnetic interaction J is larger than the antiferromagnetic one ($J'/J > -1$). For dominant antiferromagnetic interactions along the diagonal of the rhomb, intermediate spin states are observed. Thus, in the range $-2 < J'/J < -1$, the cluster has an $S = 3$ ground spin state, while, for values of $J'/J < -2$, the ground spin state is a mixture of spin states with $S = 2$, 1, and 0. In the present case the two interactions are ferromagnetic ($J'/J \approx 0.42$,

(20) Gladfelter, W. L.; Lynch, M. W.; Schaefer, W. P.; Hendrickson, D. N.; Gray, H. B. *Inorg. Chem.* **1981**, *20*, 2390.

(21) The presence of paramagnetic impurities does not imply the existence of a Mn^{II} as a counterion replacing two Na^+ ions (as in the Cu^{II} derivative). It seems more probably that a partial decomposition of the tetramer gives rise to mono- and trisubstituted Dawson–Wells structures, which will be responsible of the paramagnetic impurities, but leaving the total number of Mn^{II} ions equal to four per mol. This decomposition does not take place in the single crystal used for the structure determination as it was sealed with its mother liquor in a Lindemann glass capillary. This reorganization of the substituted Keggin and Dawson–Wells structures has already been observed in other related compounds.

(22) Smit, J. J.; Nap, G. M.; de Jongh, L. J.; van Ooijen, J. A. C.; Reedijk, J. *Physica* **1979**, *97B*, 365.

Table 5. Selected M–M Distances and M–O–M Angles within the Tetrameric Clusters M_4O_{16} of the Series $[M_4(H_2O)_2(XW_9O_{34})_2]^{10-}$ (M = Co^{II}, Mn^{II}, Cu^{II}, X = P; M = Zn^{II}, X = As; M = Cu^{II}/Fe^{III}, X = Fe^{III}) and $[M_4(H_2O)_2(P_2W_{15}O_{56})_2]^{16-}$ (M = Mn^{II}, Zn^{II}, and Cu^{II})

	distances (Å)			angles (deg)					
M	d(1–2)	d(1*–2)	d(2–2*)	α	β	γ	θ	ω	ref
Co^{II}	3.164	3.192	3.304	100.5	93.8	97.0	92.6	102.6	6d
Zn^{II}	3.243	3.248	3.455	99.6	96.5	103.5	94.8	101.2	6d
Mn^{II}	3.290	3.292	3.446	99.6	91.6	95.5	91.3	100.5	7e
Cu^{II}	3.247	3.259	3.080	97.7	89.2	97.6	89.6	98.3	6f
$Cu^{II}Fe^{III}$ [a]	3.127	3.144	3.079	91.4	102.4	101.6	100.6	91.0	9
Mn^{II} [b]	3.287	3.289	3.352	99.8	94.3	96.4	95.2	99.2	this work
Zn^{II} [b]	3.181	3.198	3.25	98.9	93.7	96.4	93.5	98.2	6g
Cu^{II} [b]	3.196	3.216	3.054	95.3	91.8	97.4	90.3	94.0	6f

[a] In this compound the cluster is formed by two Cu^{II} (2 and 2*) and two Fe^{III} atoms (1 and 1*). [b] In the series $[M_4(H_2O)_2(P_2W_{15}O_{56})_2]^{16-}$. In the related trimeric cluster Ni_3O_{13} in the compound $K_6Na[Ni_3(H_2O)_3PW_{10}O_{39}H_2O]\cdot 12H_2O$ the distances (Å) and angles (deg) are[11] d(1–2) = 3.178, d(2–3) = 3.177, d(1–3) = 3.172, α = 100.7, β = 92.0, θ = 92.3, θ = 91.9, ω = 100.4, and ϕ = 101.0 (see scheme below). The distances and angles are displayed in the scheme below, where small circles locate oxygen atoms and the metallic centers 1* and 2* are related to 1 and 2, respectively, by the inversion center in the tetrameric center:

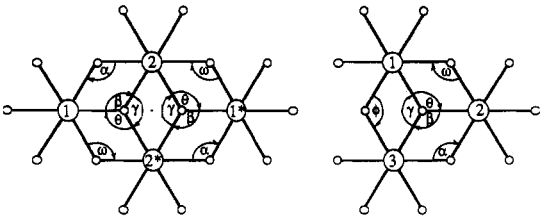

vertical line in Figure 5), so that the S = 4 state is the ground spin state being separated from the first excited state (S = 3) by $4J$ (33.2 cm^{-1}).

Although the related tetrameric Ni^{II} cluster of the $[M_4(H_2O)_2(PW_9O_{34})_2]^{10-}$ series has not been obtained, these exchange parameters can be compared to those obtained in a similar trinuclear cluster encapsulated between a trivacant Keggin fragment $[PW_9O_{34}]^{9-}$ and a $[WO_6]$ octahedron ($J = J'$ = 2.9 cm^{-1}).[11] In both cases the NiO_6 octahedra are sharing edges in a similar way leading to similar Ni–O–Ni angles and Ni–Ni distances (in fact, the Ni_3O_{13} cluster can be seen as a fragment of the Ni_4O_{16} cluster). As can be seen in Table 5, the polyoxometalate fragments impose M–O–M angles ranging from 94 to 100°. These angles are in the range in which the Ni–Ni ferromagnetic exchange pathways are dominant (90 ± 14°). In this context it should be noted that other nickel ferromagnets are known. But in contrast with compound **2**, all these complexes show a cubane-type framework and significant intercluster interactions. It is interesting that despite the structural differences, the rhomblike cluster has an exchange coupling similar to those reported in the cubane clusters (3–11 cm^{-1}). Finally, the smaller (absolute) value of J' compared to J (in both Mn and Ni compounds) may be related to the larger M–M distance for the diagonal of the rhomb (3.35 Å compared to 3.29 Å for the side of the rhomb). This situation is reversed for the Cu compound as a consequence of the Jahn–Teller distortion of the CuO_6 sites, which are axially distorted in such a way that the long axes of the four octahedra are parallel; as a result, the M–M distance for the diagonal of the rhomb is shorter (3.05 Å compared to 3.20–3.22 Å for the side of the rhomb) and a stronger value of J' compared to J is observed (J'/J = 3.6).

Conclusions

We have reported here two new members (M = Ni^{II} and Mn^{II}) of the series $[M_4(H_2O)_2(P_2W_{15}O_{56})_2]^{16-}$. The solved structure of the Mn^{II} derivative, a new example of this series where no Jahn–Teller distortions for the M sites are present, has allowed us to confirm the changes induced into the polytungstate framework as a result of the Jahn–Teller distortions found by Weakley and Finke in the Cu_4O_{16} entity.

On the other hand, the rigidity imposed by the polytungstate ligand has guaranteed the typical rhomblike geometry for the M_4O_{16} entity, emphasizing once more the ability of these ligands to isolate magnetic tetramers with very unusual geometries, which often favor ferromagnetic exchange interactions and, consequently, high ground spin states. This is the case of the Ni^{II} compound, which exhibits a ferromagnetic ground spin state S = 4, which is the largest one reported in a heteropoly complex.

Acknowledgment. This work is supported by The Dirección General de Ciencia y Tecnología (DGICYT Grant PB91-0652), The Caja de Ahorros del Mediterráneo and The European Union (Network on Molecular Conductors and post-doctoral grants to C. J. G.-G. and J.J.B.-A.).

Supplementary Material Available: Tables giving the values of S, S', S'', E_i, a_i, and b_i for the 146 spin states in a Mn^{II} tetramer (Table S1) and for the 19 spin states in a Ni^{II} tetramer (Table S2) and for $Na_{16}[Mn_4(H_2O)_2(P_2W_{15}O_{56})_2]\cdot 53H_2O$ (**1**) tables giving data and details of the structure determination, complete bond lengths and angles, and anisotropic thermal parameters (Tables S3–S6) (10 pages). Ordering information is given on any current masthead page.